Toward an Understanding of the Role of Dynamics on Enzymatic Catalysis in Lactate Dehydrogenase†

Miriam Gulotta,‡ Hua Deng,‡ Hong Deng,‡ R. Brian Dyer,§ and Robert H. Callender*,‡

Department of Biochemistry, Albert Einstein College of Medicine, Bronx, New York 10461, and Bioscience Division, Mail Stop J586, Los Alamos National Laboratory, Los Alamos, New Mexico 87545

Received December 5, 2001; Revised Manuscript Received January 14, 2002

ABSTRACT: The motions of key residues at the substrate binding site of lactate dehydrogenase (LDH) were probed on the 10 ns to 10 ms time scale using laser-induced temperature-jump relaxation spectroscopy employing both UV fluorescence and isotope-edited IR absorption spectroscopy as structural probes. The dynamics of the mobile loop, which closes over the active site and is important for catalysis and binding, were characterized by studies of the inhibitor oxamate binding to the LDH/NADH binary complex monitoring the changes in emission of bound NADH. The bound NAD-pyruvate adduct, whose pyruvate moiety likely interacts with the same residues that interact with pyruvate in its ternary complex with LDH, served as a probe for any relative motions of active site residues against the substrate. The frequencies of its C═O stretch and $-COO^-$ antisymmetric stretch shift substantially should any relative motion of the polar moieties at the active site (His-195, Asp-168, Arg-109, and Arg-171) occur. The dynamics associated with loop closure are observed to involve several steps with motions from 1 to 300 μs. Apart from the "melting" of a few residues on the protein's surface, no kinetics were observed on any time scale in experiments of the bound NAD-pyr adduct although the measurements were made with a high degree of accuracy, even for final temperatures close to the unfolding transition of the protein. This is contrary to simple physical considerations and models. These results show that, once a productive protein/substrate complex is formed, the binding pocket is very rigid with very little, if any, motion apart from the mobile loop. The results also show that loop opening involves concomitant movement of the substrate out of the binding pocket.

Our picture of the molecular nature of enzymatic catalysis typically revolves around static structures of enzymes, with and without bound substrates and inhibitors, as determined from crystallographic, multiple dimension NMR, or vibrational spectroscopy. This is necessarily a limited view, providing only "snapshots" of the development of the reaction coordinate and providing no sense of the timing of various events. Indeed, the theory of transition state stabilization, invoked to explain the observed rate enhancements produced by enzymes over the corresponding chemical reactions in solution, is also a static picture. Modern paradigms for enzymatic catalysis can and do include atomic motion; however, little experimental data support these theories. A basic reason for the paucity of an experimental understanding has to do with technical limitations. It has, until recently, been very difficult to observe atomic motion on the 10 ns to 1 ms time scales. Here, we apply laser-induced temperature-jump relaxation spectroscopy to study aspects of the dynamics occurring at the active site of lactate dehydrogenase. Laser light tuned to the near-IR is used to irradiate weak water bands. The subsequent thermalization of the excited water molecules results in a prompt temperature increase, as fast as picoseconds. Temperature jumps can provide the "trigger" initiating a reaction or conformational change, and the conformational change can be monitored by a number of spectroscopies. In this study, we measure both tryptophan and NADH fluorescence as well as absorbance in the mid-IR.

Lactate dehydrogenase (LDH;[1] EC 1.1.27) accelerates the reduction of pyruvate by NADH to lactate and NAD^+ by about 10^{14}-fold relative to the corresponding model reaction (*1*). The reaction involves the direct transfer of a hydride ion from C4 of the reduced nicotinamide group of NADH to the C2 carbon of pyruvate (Figure 1). The nature of the LDH/NADH/pyruvate (ternary) complex has been studied using an adduct complex, LDH/NAD-pyr, that is formed by the addition of the C3 carbon of the pyruvate enol to the C4 position of the nicotinamide ring of NAD^+ in the presence of LDH (*1*). The dissociation constant for the adduct is about 10^{-10} M, just slightly smaller (about a factor of 10) than the product of the dissociation constants for LDH with NADH and LDH/NADH with pyruvate. The pyruvate moiety of this

† This work was supported by the Institute of General Medicine, National Institutes of Health Grants GM53640 (R.B.D.) and GM35183 (R.H.C.), and the National Science Foundation, Grant MCB-9727439 (R.H.C.).

* Corresponding author. Phone: 718-430-3024. Fax: 718-430-8565. E-mail: call@aecom.yu.edu.

‡ Albert Einstein College of Medicine.

§ Los Alamos National Laboratory.

[1] Abbreviations: NAD^+, oxidized β-nicotinamide adenine dinucleotide; NADH, reduced β-nicotinamide adenine dinucleotide; LDH, lactate dehydrogenase; H4 LDH, H4 pig heart isozyme of LDH; NAD-pyr, adduct formed in the presence of LDH from pyruvate and NAD^+; IR, infrared; FTIR, Fourier transform infrared.

10.1021/bi016009a CCC: $22.00
Published on Web 02/09/2002

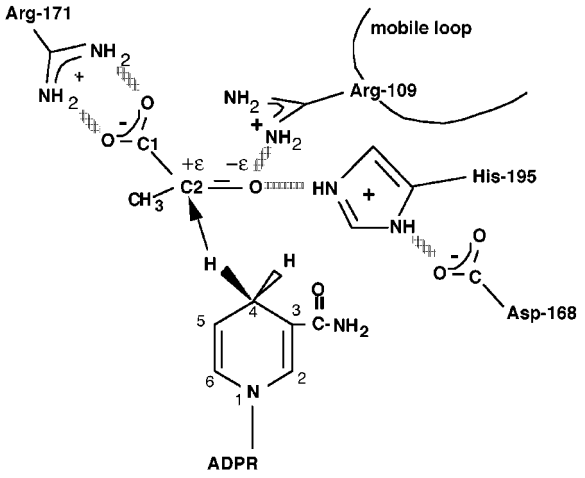

FIGURE 1: Diagram of the binding site of LDH with bound NADH and pyruvate showing hydrogen bonds between the substrate and key catalytically important residues of the protein. The catalytic event involves the hydride transfer of the C4 hydrogen of NADH from the *pro-R* side of the reduced nicotinamide ring to the C2 carbon of pyruvate and protein transfer from the imidozole group of His-195 to pyruvate's keto oxygen.

adduct likely interacts with the same residues that interact with pyruvate in its ternary complex with LDH on the basis of X-ray structural (*2*−*5*) and chemical (*1*, *6*, *7*) as well as Raman structural (*8*, *9*) studies. Oxamate (NH_2COCOO^-) is an inhibitor of LDH and is an isoelectronic and isosteric mimic of pyruvate. It too binds in a structural arrangement believed to mimic pyruvate binding. Moreover, it has been shown to have binding kinetics very similar to that of pyruvate (*10*, *11*).

While the dynamics of the catalytic reaction are largely unknown, we postulate the following crude outline of the initial dynamics of enzyme-catalyzed conversion of pyruvate to lactate. Pyruvate forms some sort of encounter complex with LDH/NADH. Once the substrate reaches positioning close enough to the enzyme's active site, which is buried into the enzyme, a loop of the polypeptide chain, residues 98−110, closes over the active site entrance, water leaves the binding pocket, the enzyme tightens around the bound substrate, and key residues are brought in close proximity to the substrate. At this point, it is probable that the structural arrangement is close to what is formed in ternary complexes observed in the crystallographic studies.

Figure 1 shows a cartoon of NADH and pyruvate and its arrangement with specific active site residues of LDH. There are several charged residues that are important for catalysis and binding. The His-195 and Asp-168 dyad are essential for catalysis. N3 of the protonated imidizole ring of His-195 approaches the carbonyl ring oxygen of pyruvate at an angle that is optimal for proton transfer which must occur in the pyruvate to lactate transformation. In addition, a strong hydrogen bond is formed between the His-195 and the substrate carbonyl oxygen that polarizes the C═O bond. The loop closure of residues 98−110 also brings Arg-109 close to the substrate carbonyl oxygen, forming another hydrogen bond. It is known that electrostatic stabilization of the transition state in the pyruvate−lactate interconversion, which contains a highly polarized carbonyl moiety, $^+C-O^-$, is responsible for about half of the rate enhancement brought about by LDH (*1*, *9*). The enzyme-induced carbonyl bond polarization shows up as a downward frequency shift in the C═O stretch mode (located at 1710 cm^{-1} in solution) of 35 cm^{-1} (*9*). It has been determined that the His-195/Asp-168 dyad is responsible for about 24 cm^{-1} of this frequency shift and Arg-109 for about 11 cm^{-1}. Another key residue is Arg-171, which solvates the ionized carboxylic moiety of pyruvate at the binding site; this interaction affects the stretch modes of the ionized carboxyl moiety, raising its antisymmetric stretch frequency by 20 cm^{-1} (1615 to 1635 cm^{-1}; see below).

We use the NAD-pyr adduct as a probe of the dynamics taking place at the active site. This molecule does not undergo catalysis, and it does not dissociate from LDH. It is different from the normal ternary productive complex in that the NADH cofactor and the pyruvate substrate are tied together through the covalent bond between the C4 position of NADH and the C2 carbon of pyruvate. Hence, any relative motion between these normally reacting species is frozen out. This simplifies the system to a point where several important questions concerning specific dynamical features of the active site can be answered.

The central issue we pose in this study is, once pyruvate is bound to LDH, what are the relative motions of the key residues in the protein binding pocket with respect to the bound substrate? The dynamics of loop opening/closing are of particular interest. Holbrook and colleagues (*10*, *11*), in kinetic studies of substrate and inhibitor binding to LDH/NADH, have shown that the loop opening rate is 580 s^{-1} and loop closure occurs at 3020 s^{-1} at 23 °C. We have confirmed these rates in T-jump relaxation experiments of the LDH/NADH complex when it binds oxamate using the emission properties of the nicotinamide headgroup of NADH as a marker of loop open/closing. Our studies also exhibit two faster processes, showing that loop closure involves several steps. Loop motion can be monitored as well through shifts in frequency of the C═O stretch of the bound NAD-pyr adduct since, as mentioned above, the breaking and/or weakening of the hydrogen bond between Arg-109 and substrate yield(s) up to 11 cm^{-1} frequency shift in this C═O stretch. In this study, we have found it possible to determine a shift in this bond-stretching frequency of as little as 1 cm^{-1} and smaller over time scales of 20 ns to 10 ms using our IR T-jump relaxation spectrometer. Likewise, any relative motion between the His-195/Asp-168 dyad and substrate C═O moiety shows up as a substantial shift in the substrate C═O stretch frequency. Motion against the substrate's carboxyl group can be assessed by shifts in the antisymmetric stretch frequency of a $-COO^-$ moiety which lies at 1616 cm^{-1} in solution. The frequency of this band is upshifted by the formation of hydrogen bonds and salt bridges, and so the dynamics of the making/breaking of these interactions show up as frequency shifts of this internal coordinate. In this way, the relative dynamics of the substrate against its protein host can be characterized quite thoroughly and specifically.

MATERIALS AND METHODS

Materials. L-Lactate dehydrogenase (L-LDH from pig heart) was purchased as a crystalline suspension in ammonium sulfate solution from Boehringer-Mannheim Co. The

enzyme was dialyzed three times against 0.1 M sodium phosphate solution (pH 7.0) at 4 °C. After dialysis, the protein solution was filtered through a 0.45 μM filter and concentrated by centrifugation. NADH (grade I, 100%) was purchased from Boehringer-Mannheim Co. and used without further purification. Concentrations of LDH and NADH were determined using extinction coefficients $\epsilon_{280} = 200$ mM^{-1} cm^{-1} and $\epsilon_{340} = 6.22$ mM^{-1} cm^{-1}, respectively. The adduct samples used in the infrared work were prepared by adding LDH, NAD^+, and pyruvate in a 1:5:10 N ratio. The complex was allowed to form overnight. Unreacted NAD^+ and pyruvate were removed using a 2 mL Amicon concentrator (Millipore) and washing/concentrating the adduct four times with deuterated buffer. The adduct concentration was determined spectrophotometrically using $\epsilon_{325} = 2.1$ mM^{-1} cm^{-1} (*12*).

The IR difference spectrometer has been described previously (*13*). FTIR spectroscopy was performed on a Nicolet Magna-IR 760 Fourier transform spectrometer (Thermo-Nicolet, Madison, WI) using a MCT detector in each case. Both reference and sample solutions were simultaneously loaded into a dual cell shuttle accessory. CaF_2 plates with 15, 25, or 50 μm Teflon spacers were used. A two-position sample shuttle was used to alternate between the sample and reference buffer positions; this procedure substantially decreased the spectral contribution of residual water vapor after subtraction. A water vapor spectrum was also taken and was subtracted from any difference spectra until this contribution was nulled; the water vapor peaks are easily identified by their narrow bandwidths and known positions. Spectra were collected in the range of 1100−4000 cm^{-1} with 2 cm^{-1} resolution, and a Happ−Genzel apodization was applied. Omnic 4.0a (Thermo Instruments Corp.) software was used for data collection and analysis. The solvent background spectrum was subtracted from the each protein solution spectrum. Since the sample and reference cells were assembled separately, their path lengths were not exactly equal. To correct for this, the subtracted spectrum was multiplied by a correction factor, typically in the range of 0.95−1.05, adjusted until the regions that lacked the ligand spectrum were as flat as possible and the remaining peaks were reasonably symmetrical. In the case of the isotope-edited adduct spectra, the correction factor was adjusted until the background protein peaks were nulled.

Temperature-Jump Spectrometers. The essence of the kinetic spectrometer is the same for the IR and fluorescence temperature-jump instruments. A pulsed Nd:YAG laser is used to induce a 10−20 °C temperature jump in an aqueous sample. The change in signal induced by the T-jump (transmission for IR or emmitted fluorescence light) is detected in real time; hence a very accurate baseline is automatically provided, and quite small changes can be determined.

The pump pulse and IR production used for the IR studies have been previously described (*14*−*16*). This spectrometer consists of a widely tunable (from 1600 to 1700 cm^{-1}) CW lead salt infrared diode laser (Laser Analytics) that functions as the probe for the IR measurements. An injection-seeded, Q-switched Nd:YAG laser (Spectra Physics GCR4) combined with a 1 m Raman shifter filled with H_2 gas is used to produce the pump radiation at 2 μm (10 ns fwhm Gaussian pulse width), which is the source for the temperature jump. This wavelength corresponds to the peak of a weak D_2O near-IR absorption band ($\epsilon = 10.1$ cm^{-1} at 2 μm). The high transmission ensures a nearly uniform temperature profile in the approximately 14 nL ($\pi \times 100 \times 50$ μm^3) laser interaction volume. The combined total instrument response time is approximately 23 ns. The sample cell consists of a pair of CaF_2 windows separated by a 50 μm spacer. Unlike standard spacers, this one has a strip of Teflon down the middle which splits the cell into two separate compartments. This arrangement optimizes the match between the sample and reference compartments. In the IR absorption experiments, D_2O was used as solvent to shift water's strong absorption band near 1630 cm^{-1} down to 1200 cm^{-1}, which allows most of the probe light to be transmitted through the 50 μm path length cells. The pump laser energy is absorbed by water (D_2O), and the temperature of the volume of water reaches its maximum value within a response time of ca. 23 ns since temperature thermalization and diffusion within water occur on subnanosecond time scales. The diffusion of heat out of the interaction volume takes about 8 ms in our cells. The size of the T-jump was calibrated using the change of D_2O absorbance with temperature which acts as an internal thermometer in the range of 1632−1700 cm^{-1} (*14*). The T-jump was determined to within 2 °C. The system operates at 10 Hz.

The fluorescence spectrometer has also been previously described (*17*, *18*). Rapid temperature perturbation, i.e., up to a 20 °C jump here, was achieved by irradiating water (H_2O) using an IR emission at 1.54 μm with 70 mJ incident energy in a spot of about 1−2 mm diameter. This emission was produced by Raman shifting the fundamental (1.064 μm) of a Quanta-Ray GCR-150 Q-switched Nd:YAG laser (Spectra Physics, Mountain View, CA), using 1 m Raman shifter filled to 450 psi with methane gas. The pulsed laser was operated at 1 Hz. Fluorescent emission was excited by an Innova 200-25/5 argon ion laser (Coherent, Palo Alto, CA) operated multimode in the deep UV with outputs at 275 and 290 nm or at 360 nm. A shutter intercepted the excitation light and was opened only when needed (typically for about 10 ms for each pulse of the heating beam); this permitted a more intense irradiation of the chromophore while still avoiding photodamage. The excitation laser was focused on the sample with a spot of 0.3 mm diameter, which was overlapped with the near-IR pump laser spot. Fluorescent signals filtered through a narrow-band interference filter (450 ± 20 nm, used to monitor NADH emission, and 340 nm ± 12 nm for tryptophan) were acquired by a R4220P photomultiplier tube (Hamamatsu, Bridgewater, NJ) at a 50° angle toward the incident excitation beam. All signals were averaged by digitizing oscilloscopes (TDS 754A and TDS 420A, Tektronix Inc., Beaverton, OR). Approximately 100 μL solutions were needed to fill a quartz sample cell (0.2 mm path length).

RESULTS

Experiments were performed on three different protein solutions: the apoprotein, the ternary LDH/NADH/oxamate complex, and the LDH/NAD-pyr adduct complex. In general, static thermal measurements preceded the kinetic studies. This calibrates the expected signal size to be observed in the kinetic work and also sets the magnitude of the signal at infinite time in the kinetic experiments.

Apo-LDH was studied since, as will be seen below, relaxation signals resulting from the T-jump are observed that arise from the enzyme itself, in the absence of bound ligand. These signals show up as well in ligand-bound systems as a background and so need to be characterized. Loop opening/closing dynamics are a feature of the active site of LDH. As shown below, the loop motion shows up in T-jump relaxation measurements by perturbing the equilibrium between bound and unbound substrate/inhibitor from LDH/NADH. We use the inhibitor oxamate since its binding kinetics, at least concerning loop motion, are essentially identical to the substrate pyruvate and the complex does not undergo catalysis, which complicates greatly the kinetic analysis (*10*, *11*). Since the emission of the reduced nicotinamide moiety is essentially quenched for the ternary LDH/NADH/oxamate complex with the loop down but not quenched for the loop open geometry, NADH emission is a very sensitive reporter of loop closure kinetics. We report here the measurement of the binding process of oxamate to LDH/NADH using NADH fluorescence changes in response to the T-jump to verify previous studies (*10*, *11*); the results yield essentially the same kinetics of loop closure as observed previously although faster steps are additionally clearly observed. We are in the process of structurally characterizing these faster kinetic steps. The third protein system that we perform measurements on was the LDH/NAD-pyr complex. This complex allows us to probe the protein motions coupled to the substrate in the absence of other complicating processes. This complex does not undergo catalysis, the substrate does not dissociate, and the NADH cofactor and the substrate are covalently linked such that any relative motion between them is inhibited.

Apo-LDH. Figure 2a shows the IR absorbance of LDH in the amide I′ range. The solvent is pH 7 D_2O/buffer. The prime refers to deuterated amide groups which result when the exchangeable amide protons are deuterated by suspension in D_2O. A second derivative analysis (not shown) reveals that the amide I′ band essentially consists of two overlapping bands at 1656 and 1637 cm^{-1}. The value of 1656 cm^{-1} is characteristic of α-helical secondary structure while the 1637 cm^{-1} band can be assigned to β-sheet and/or solvated helix. A sample at a concentration of 497 μN (as determined from its UV absorption at 280 nm) was measured at several different path lengths from 15 to 100 μm in order to obtain the absorption constant at the peak position in the IR. This procedure minimizes the error induced by the solvent background in the calculated protein extinction coefficient. At 1652 cm^{-1}, the maximum of the amide I′ band, we find that $\epsilon_{1652} = 15.1\ N^{-1}\ \mu m^{-1}$ ($6.03\ 10^{-5}\ M^{-1}\ cm^{-1}$). Figure 2b shows the temperature dependence of the amide I′ spectrum by calculating a series of "double difference" curves. At each temperature, the residual D_2O background and water vapor bands have been subtracted from the sample spectrum. The absorbance spectrum at 10 °C is subtracted from these background-adjusted absorbance bands at successively higher temperatures. The pig heart LDH used in this study is a tetramer with each of the four binding sites acting independently. In this paper, we use the units of "normality" to indicate the molarity of binding sites, as has been customary. The double difference curves show a loss of absorbance peaked at 1625 cm^{-1} and a concomitant gain of absorbance peaked near 1667 cm^{-1}. A plot of the difference in absorbance at any wavenumber between 1625 and 1667 cm^{-1} divided by the peak absorbance of the protein's amide I′ band (near 1652 cm^{-1}) as a function of temperature yielded a linear response over the entire temperature range studied with a slope of 0.00224 ($\pm 5.55 \times 10^{-5}$) $°C^{-1}$.

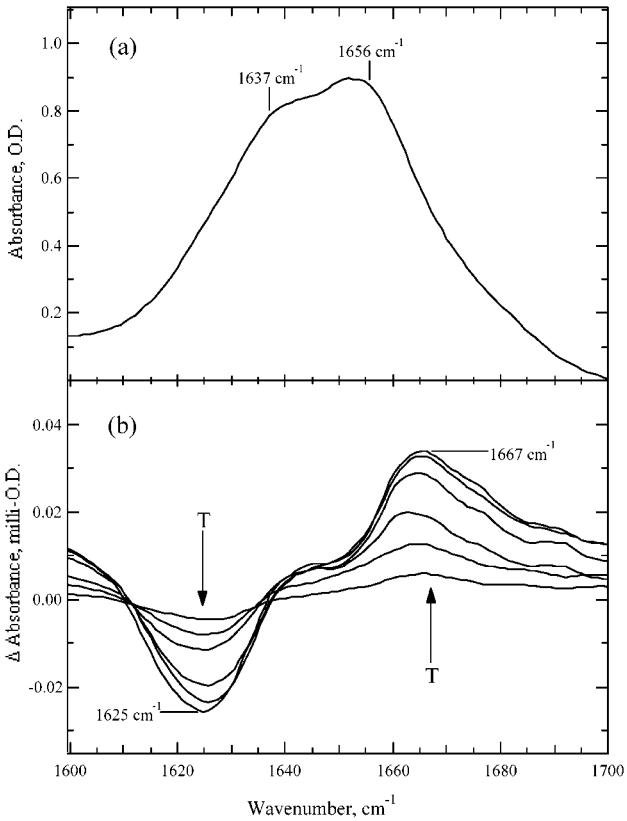

FIGURE 2: (a) IR absorbance band of LDH in D_2O. The concentration of the sample is 1.2 mN, cell path length is 50 μm, and uncorrected pH = 7.2, at 25 °C. A second derivative analysis reveals that the amide I′ is composed of two bands at 1637 and 1657 cm^{-1}. The maximum of the amide I′ lies at 1652 cm^{-1}. (b) Difference spectra generated by subtracting the spectrum at 10 °C from the spectra taken at 20, 25, 29, 34, 39, and 44 °C. The changes are monotonic with temperature and go in the indicated direction. As temperature increases, a gain in intensity is observed peaked at 1667 cm^{-1} with a concomitant loss at 1625 cm^{-1}.

The type of melting behavior exhibited in Figure 2b is very similar to studies involving the melting of "solvated" helices (see e.g., ref *14*). The characteristic frequency of helical model peptides in solution and solvated helices of proteins lies between 1625 and 1640 cm^{-1}. When this helix melts, producing random coils, the characteristic amide I′ frequency lies near 1665 cm^{-1}. An apparent linear response of the melting, rather than sharp transitions that are normally produced by the melting of proteins, is also found in melting studies of helical peptides. This is because the enthalpy difference between the folded and unfolded portion of the helical peptide involves few residues and is therefore small. Hence, it is reasonable to assign, tentatively, the behavior observed in panel b of Figure 2 to the melting of a few amide residues, probably on the surface of the protein,. Assuming, crudely, that the amide I′ C═O stretch modes of each of the 331 residues (per subunit of the tetramer) contribute equally to the IR absorbance and that each has a half-width of 10 cm^{-1}, about 83 residues contribute to the intensity at any

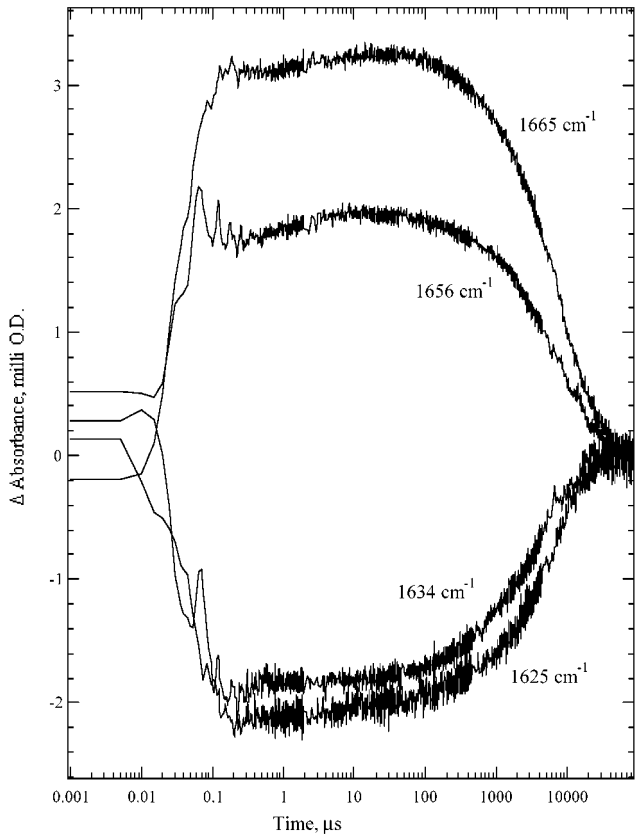

FIGURE 3: Kinetic IR response of apo-LDH in D_2O for a T-jump from 11 to 23 °C at four different frequencies: 1625, 1634, 1656, and 1665 cm^{-1}. The background D_2O response has been subtracted from these data. All curves show a slow recovery on the millisecond time scale since heat flows out of the laser interaction volume with a ca. 8 ms time constant returning to the original temperature of 11 °C. The sample concentration was 80 μN, in 100 mM deuterated sodium phosphate buffer, uncorrected pH* = 7.2, and a cell path length of 100 μm (optical density = 116 mOD at 1657 cm^{-1}).

point across the amide I′ band which is about 40 cm^{-1} broad. At 1625 cm^{-1}, a 10 °C change in temperature corresponds to a change of 11 mOD, and the 83 residues yield an absorbance of 460 mOD (all for the concentrations and path length of Figure 2). Hence, it is estimated that about 2 residues melt for a 10 °C temperature change. This simple calculation demonstrates that IR spectroscopy can easily detect structural changes in a few residues within a large protein complex. Similar sensitivity of infrared spectroscopy to small changes in local structure within a large protein (e.g., a single chemical bond within bovine cytochrome *c* oxidase, MW > 220 kDa) has been demonstrated previously (*19*).

Figure 3 shows the relaxation kinetics of apo-LDH probed at several wavelengths in the amide I′ spectral range in response to a T-jump from 11 to 23 °C. Since D_2O has a small absorbance at these wavelengths which is temperature dependent, there is a substantial response from D_2O/buffer alone. The traces presented result from a subtraction between the sample transient (D_2O/buffer/protein) and the reference transient (D_2O/buffer alone). The response of the reference provides the calibration of the magnitude of the T-jump and also yields the instrument temporal response function since the thermalization of the absorbed laser light occurs essentially instantaneously (ca. 10 ps). The late time response occurring past 1 ms results from the higher temperature in the laser interaction volume returning to its initial value (diffusional cooling), which has a time constant of about 8 ms in the IR spectrometer. This response is driven solely by the cooling dynamics and contains no information regarding the protein dynamics. As is apparent, there is a very sudden early time bleach at wavelengths around 1630 cm^{-1} and a concomitant gain in intensity at wavelengths near 1665 cm^{-1}. The apparent rise time of this sudden response is just slightly longer than the 23 ns response time of the instrument, at 37 ns. Convolving the exponential instrument response ($\tau = 23$ ns) with a single-exponential rise describing the protein response yields a best fit with $\tau = 30$ ns for the protein response. The absorbance magnitude in the observed changes in the 37 ns transient between 1665 and 1625 cm^{-1} in response to a T-jump of 12 °C is close to that predicted (5 mOD for both cases) from the static melting measurements (Figure 2b). Previous studies have shown that the characteristic relaxation behavior of solvated helices in response to a T-jump is a single-exponential response with a lifetime of 30−150 ns (*14*, *16*, *20*). Hence, the dynamical nature of the changes in IR absorbance as a function of temperature observed in the static data of Figure 2b is in agreement with assigning this to the melting of a small number of solvated helices. In Figure 3, very small amplitude signal kinetics on the 1−10 μs time scale are suggested. These were found to be irreproducible and are likely artifacts introduced by a small incomplete subtraction between the sample and reference transients. Since the entire magnitude of the static IR absorbance is manifested in the 37 ns signal, it is unlikely that there is any kinetic response occurring slower than the 8 ms cooling time. Hence, the only kinetics observed from apo-LDH as observed using IR probes of structure is the prompt 37 ns early time kinetics.

Figure 4 shows the emission of the indole rings of the tryptophan residues in LDH as a function of time after the T-jump. The early prompt negative signal is unresolved and is due to the sudden temperature increase since increasing temperature generally quenches fluorescence emission. It is possible that some of this initial transient may arise as well from sub-15 ns changes in structure of the protein. As in the IR experiments, the emission increase observed past 1 ms is due to diffusion of heat out of the laser interaction volume, producing sample cooling. The early time kinetics are fitted to a three-exponential function with time constants of 12 and 17 ns and 3.5 μs; the fit is overlaid on the data. The 12 ns transient is the instrument response. Two resolved transients are then observed in the kinetics of Figure 4: emission recovery with a time constant of 17 ns and an emission decrease occurring at 3.5 μs. It seems reasonable to associate the nanosecond kinetics observed in the IR T-jump kinetics (Figure 3), and the structural change responsible for these signals, to the 17 ns transient observed in the Trp emission kinetics since the relaxation times match approximately to within our errors. We have no structural explanation of the 3.5 μs transient.

LDH/NADH + Oxamate. Holbrook and co-workers performed T-jump relaxation experiments and stopped-flow mixing studies on the kinetics of loop closure in response to binding the inhibitor oxamate (*11*) and the substrate pyruvate (*10*) to LDH/NADH but on slightly modified proteins. LDH with Tyr-237 nitrated produces a visible absorption center

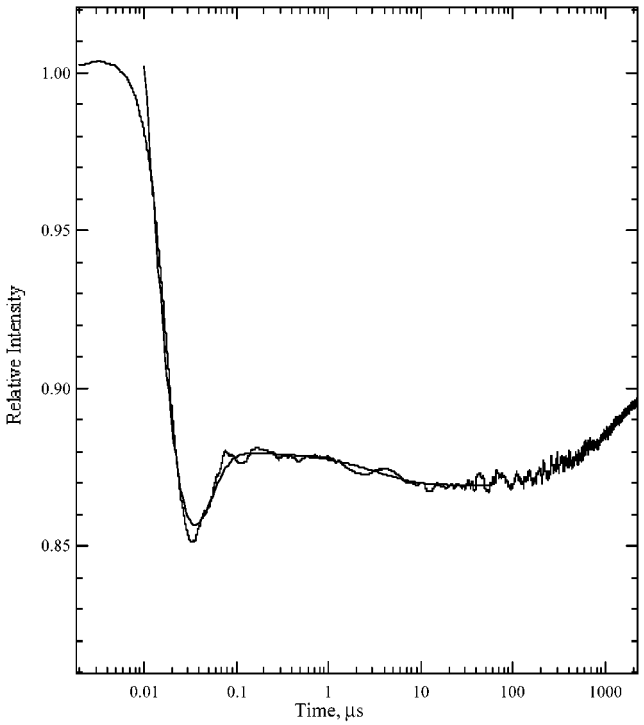

FIGURE 4: Kinetics of the Trp emission of apo-LDH measured at 340 nm in response to a T-jump from 10 to 26 °C. The early time kinetics were fitted to a three-exponential function with time constants of 12 and 17 ns and 3.5 μs, which is overlaid on the data. The emission kinetics show a slow recovery on the millisecond time scale from heat diffusion out of the laser interaction volume returning to the original temperature of 10 °C. The protein concentration was 100 μN in 100 mM sodium phosphate, pH = 7.2.

sensitive to loop closure; in some studies, DMSO/water mixtures at temperatures below 0 °C were used to slow the rates of loop motion to the point where conventional stopped-flow devices could monitor the process. The results were fit to a kinetic model which incorporated the protein mobile loop closing over the bound inhibitor (or substrate), as shown in Scheme 1. In this scheme, k_{closed} and k_{open} are the rates of loop closure and opening, respectively, and LDH^{open} and LDH^{closed} denote protein with the loop open or closed. The analysis assumes that the initial bimolecular collision process is fast, followed by a slower unimolecular rearrangement. By varying the amount of free oxamate and the binary complex, LDH/NADH, the following rates were derived: $K = k_{off}/k_{on} = 0.156$ mN, $k_{closed} = 580$ s^{-1}, and $k_{open} = 3020$ s^{-1}, at a final temperature of 23 °C. At high concentration of free inhibitor, the observed relaxation time is the sum of the forward and backward unimolecular rearrangement, $k_{closed} + k_{open} = 3600$ s^{-1}. An Arrhenius analysis of the observed rates of loop closure yielded an activation energy of 33 kJ/mol (*10*). We have performed similar T-jump studies near 20 °C and found rates quite close to those reported previously (*11*). Our studies, however, report the emission of the reduced nicotinamide ring of NADH and native LDH. Fluorescence from NADH is strong in the LDH/NADH binary complex, where it is believed that the loop is in an open conformation, to almost completely quenched upon formation of the ternary LDH/NADH/oxamate complex with the loop closed. Hence, substantial changes are expected when the loop closes down over the inhibitor and cofactor.

Scheme 1

$$\text{LDH/NADH} + \text{oxamate} \underset{k_{off}}{\overset{k_{on}}{\rightleftharpoons}} \text{LDH}^{open}\text{/NADH/oxamate} \underset{k_{open}}{\overset{k_{closed}}{\rightleftharpoons}} \text{LDH}^{closed}\text{/NADH/oxamate}$$

Figure 5 shows the emission of NADH in response to a T-jump of 21 °C from 20 to 41 °C. Following the kinetic model above, the large amplitude increase in emission with a time constant of 119 μs corresponds to the relaxation time of loop closure, $k_{closed} + k_{open}$. This is in good agreement with the extrapolated value (75 μs) to 41 °C using an Arrhenius function with a loop motion activation energy of 33 kcal/mol and a rate of 3600 s^{-1} at 23 °C. In addition, the observed emission increase with increasing time is physically consistent with the step corresponding to loop motion. The sudden temperature increase results in driving the system toward a decrease of the fluorescence-silent LDH^{closed}/NADH/oxamate complex and an increase of presumably fluorescent LDH^{open}/NADH/oxamate and LDH/NADH binary complex, i.e., a change from right to left in Scheme 1.

The emission kinetics shown in Figure 5 were fit to exponential functions in time, $A_n \exp(\tau/\tau_n)$. In addition to the 119 μs relaxation time, the data require two other relaxation times to fit the data. All together, $\tau_n = 1.5$, 53, and 119 μs. It is unclear as to what these faster times correspond in structural terms, but their existence implies that loop dynamics of LDH are more complicated than as simply represented by the kinetics shown in Scheme 1. We are in the process of performing studies to probe the structural basis of these faster times. For now, we note simply that the binding dynamics of NADH to LDH involves quite complicated dynamical motions over a wide range of time scales (*17*) so perhaps it is not unexpected that the dynamics of binding oxamate to LDH/NADH might be more complicated than can be represented in a single unimolecular conformational change.

LDH/NAD-pyr Adduct Complex. The first set of experiments on the adduct complex are aimed at measuring the positions and cross sections in the IR of the ketone's C═O stretch and the antisymmetric $-COO^-$ stretches of the adduct. We wish to measure changes in these parameters when the LDH/NAD-pyr adduct complex is perturbed by the T-jump in transient IR transient experiments, and so the position and absorbance as a function of temperature in static measurements must be characterized if the transient results are to be interpreted. The experiments are not easy since both modes lie in a spectrally congested region. The C═O stretch mode actually lies within the protein's strong amide I′ band. Our approach is to employ isotope editing coupled with highly accurate difference spectroscopy. In brief, the IR spectra of two protein solutions, one labeled with a stable isotope which shifts the desired mode and one not labeled (at natural abundance), are measured, and the difference spectrum is calculated. All IR absorbance bands not affected by the isotope cancel out, leaving only the desired absorbance bands, which show up as positive/negative band couplets. We have previously performed isotope-edited IR difference spectroscopy on protein solutions to measure phosphate stretch modes (*13*), and the instrument and procedures are more fully discussed in Materials and Methods. The most

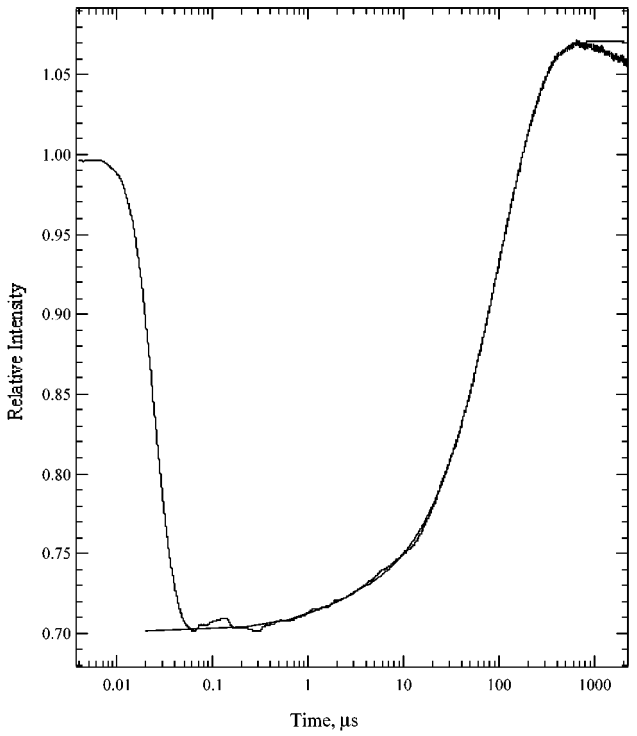

FIGURE 5: Kinetic response of NADH emission at 450 nm stimulated by energy transfer from excited Trp residues as a result of a T-jump from 20 to 41 °C for the reaction of LDH/NADH with oxamate. The kinetics were fitted to a three-exponential function with time constants of 1.5, 53, and 119 μs, which is overlaid on the data. The equilibrium intensity at 41 °C relative to 20 °C is 1.17 as determined in a separate static measurement. The emission kinetics show a slow recovery on the millisecond time scale from heat diffusion out of the laser interaction volume returning to the original temperature of 20 °C, and this obscures reaching the equilibrium position at long times. The relative initial concentrations of LDH, NADH, and oxamate were 100, 200, and 500 μN, respectively. All samples were in 100 mM sodium phosphate, pH = 7.2.

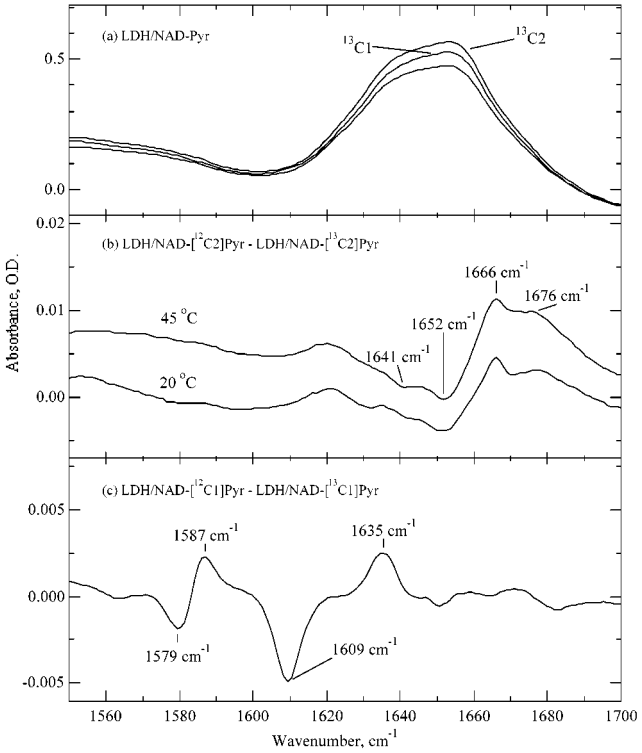

FIGURE 6: (a) Absorption of three LDH/NAD-pyr adduct complexes, LDH/NAD-pyr (natural abundance), LDH/NAD-[^{13}C1]pyr (labeled ^{13}C1), and LDH/NAD-[^{13}C2]pyr (labeled ^{13}C2), in 5 mM deuterated sodium phosphate buffer, pH* = 7.2, into 15 μm path length. The exchangeable hydrogens of the three samples have been thoroughly exchanged for deuterons. (b) Difference spectra obtained by subtracting the LDH/NAD-[^{13}C2]pyr spectrum from that of LDH/NAD-pyr at 20 and 45 °C. The amplitude of one spectrum was adjusted slightly to compensate for the small difference in concentration between the two samples (see text), and a flat baseline was added to facilitate graphical presentation. (c) Difference spectra obtained by subtracting the LDH/NAD-[^{13}C1]pyr spectrum from that of LDH/NAD-pyr at 20 °C.

difficult part of this experiment is producing balanced samples, particularly with regard to deuteron exchange of the same number of exchangeable protons. An amide I′ mode is somewhat shifted when an amide −NH group is deuterated, and this shows up in the difference spectrum if the corresponding reference amide is not likewise deuterated since the sensitivity here is better than one C═O stretch. Long exchange times were employed (see Materials and Methods) to achieve properly balanced samples.

Figure 6a shows the LDH/NAD-pyr spectrum over the 1550−1700 cm^{-1} region. Three curves are shown: the natural abundance complex (essentially all ^{12}C), the ^{13}C1-labeled complex, and the ^{13}C2-labeled complex (the numbering scheme is defined with respect to the pyruvate moiety). The difference spectra between LDH/NAD-pyr minus LDH/NAD-[^{13}C2]pyr taken at 20 °C and at 45 °C are shown in Figure 6b. There are two bands that are associated with motion of the C═O stretch: at 1676 cm^{-1}, which, judging from the matched IR intensity for the ^{13}C2 sample, shifts down 35 cm^{-1} to 1641 cm^{-1}, and at 1666 cm^{-1}, which shifts 14 cm^{-1} to 1652 cm^{-1}. The same pair of bands has been observed for the LDH/NAD-pyr adduct complex using Raman difference techniques (*8*, *9*). We have previously assigned these two bands to stretch motions of the NAD-pyr adduct's C═O group and C═C stretch motions located on the reduced nicotinamide ring. These motions are coupled in the adduct complex. The 1676 cm^{-1} band in the NAD-pyr adduct is composed mostly of C═O stretch since its shift upon ^{13}C2 substitution of 35 cm^{-1} is close to what is expected from a "pure" uncoupled >C═O stretch (39 cm^{-1} in pyruvate in solution). The 1666 cm^{-1} band contains significant C═O stretch character but relatively small 14 cm^{-1} shift upon ^{13}C2 substitution, suggesting that this mode extends substantially into C═C motions located on the nicotinamide ring (*8*). The C═O stretch of pyruvate in solution lies at 1710 cm^{-1} (*8*). Hence, the C═O bond is polarized when pyruvate binds to LDH, and this shows up in a 34 cm^{-1} downward shift in frequency of the C═O stretch from 1710 cm^{-1} in solution to 1676 cm^{-1} in the adduct complex. The 34 cm^{-1} downward shift in frequency of the C═O stretch mode has been previously extensively characterized and has important implications for the molecular understanding of LDH's catalytic mechanism (*9*). In particular, the 34 cm^{-1} shift corresponds to a $10^{5.5}$ rate enhancement of the reaction catalyzed by LDH relative to the same reaction in solution. The peak absorption cross section of the primarily C═O stretch mode of the bound NAD-pyr adduct is several times larger than the corresponding C═O stretch of pyruvate in solution. This could come about for several reasons: protein induced bond polarization, which would increase the dipole

moment of the stretch motion; mixing with C═C motions on the nicotinamide moiety; and band narrowing that typically occurs when small molecules bind to proteins. Note that neither the absorption cross section nor the band position is particularly dependent on temperature, as expected. Hence, any changes produced in the T-jump measurements at these frequencies must come about because of a changing population of the 1676 cm^{-1} species.

Figure 6c shows the LDH/NAD-pyr minus LDH/NAD-[^{13}C1]pyr difference spectrum. The 1635/1609 cm^{-1} difference couplet can be assigned to the antisymmetric stretch mode of the $-COO^-$ moiety of the bound adduct. In measurements of pyruvate in solution, this mode lies at 1616 cm^{-1} and shifts 46 cm^{-1} to 1570 cm^{-1} upon ^{13}C1 labeling (data not shown). The magnitude of the IR absorbance, the shift upon ^{13}C1 labeling, and the position of the 1635/1609 cm^{-1} difference couplet confirm the assignment. The upward shift in frequency of the antisymmetric $-COO^-$ stretch when pyruvate binds to LDH as the NAD-pyr adduct is a result of interactions at the active site. The dominant interaction is probably the salt bridge formed between the carboxyl group and Arg-171 (see Figure 1), and this interaction would lead to an upshifted frequency, as observed. The 19 cm^{-1} shift when pyruvate binds to LDH is quite large and represents a strong electrostatic interaction (*21*). The 1587/1579 cm^{-1} difference couplet is of unknown origin. There are no such bands in the spectra of pyruvate in solution; however, the mode that is responsible for this spectral feature must involve motions of the $-COO^-$ moiety. The small 8 cm^{-1} shift upon ^{13}C1 labeling suggests that this mode is extended, perhaps coupling with the C═C stretches of the nicotinamide-like headgroup of the NAD-pyr adduct. (The actual shift in frequency is almost certainly smaller than 8 cm^{-1} since the mode's bandwidth is likely comparable in magnitude to the isotope shift; in this case, the apparent shift is larger than the actual shift.)

Figure 7 shows the relaxation kinetics of the LDH/NAD-pyr adduct probed at several wavelengths in the amide I′ spectral range in response to a T-jump of 10−30 °C. As in the analogous experiments on the apoprotein (Figure 3), the transients presented in Figure 7 result from a subtraction between D_2O/buffer containing the protein and D_2O/buffer alone. The transients for the LDH/NAD-pyr adduct are essentially the same as those found for apo-LDH. The initial rise time of the transients is barely resolved at 40 ns (which includes the 23 ns instrument response), essentially the same as found in kinetic response of the apoenzyme (Figure 3). The observed absorbance changes of the initial fast response as a function of wavelength follow the static double difference curves of the apoenzyme (Figure 2). Like the apo-LDH data, the difference in magnitude of the initial rapid change for the runs at 1665 and 1625 cm^{-1} (26 mOD) is what is very close to that predicted (30 mOD) from the static double difference curves of Figure 2 for a temperature change of 20 °C and an amide I′ absorbance peak of 0.67 OD, the conditions of Figure 7. The small responses observed near 200 ns, particularly prominent in the 1651 cm^{-1} data, were not reproducible as is clear from the data in Figure 7. Their temporal response is just what is expected when occasional cavitations in the sample cells accompany T-jump experiments; we believe these signals are small cavitation artifacts. Hence, the response kinetics of the LDH/NAD-pyr adduct

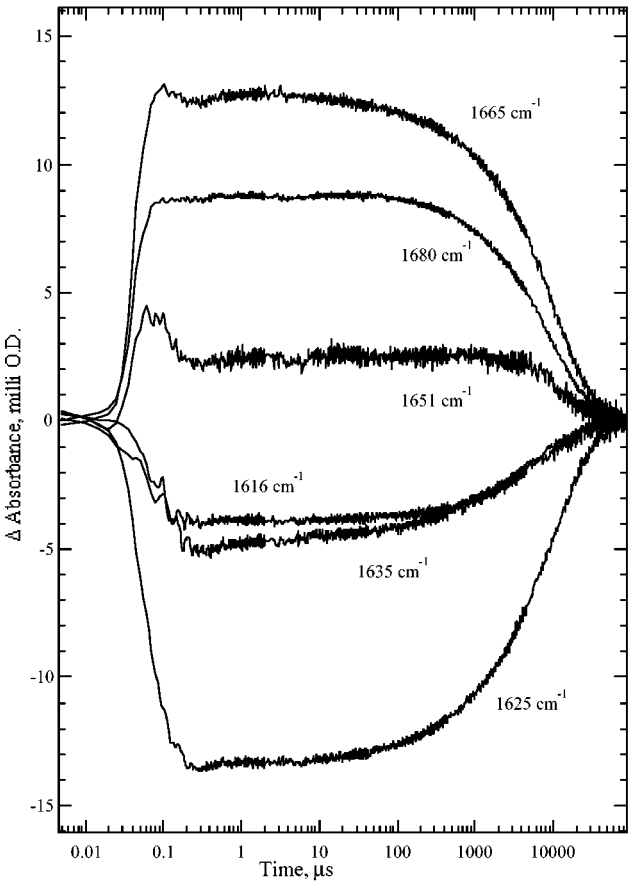

FIGURE 7: Kinetic IR response of LDH/NAD-pyr in D_2O for a T-jump from 10 to 30 °C at six different frequencies: 1616, 1625, 1635, 1651, 1665, and 1680 cm^{-1}. The background D_2O response has been subtracted from these data. All curves show a slow recovery on the millisecond time scale since heat flows out of the laser interaction volume with a ca. 8 ms time constant returning to the original temperature of 10 °C. The sample concentration was 460 μN in 5 mM deuterated sodium phosphate buffer, pH* = 7.0, and a cell path length of 100 μm.

to a T-jump, as monitored in the IR, is the same as that of the apoprotein.

To examine if there is any time dependence of the frequency of the LDH/NAD-pyr adduct carbonyl, C═O stretch, or the antisymmetric stretch mode of the $-COO^-$ moiety induced by the T-jump, the IR laser incident on the sample was set to various frequencies on or near the frequencies observed for these groups when bound to LDH (Figure 6). To maximize signal to noise, concentrated solutions were used. Also, the path length of the IR cells in the T-jump spectrometer was set to approximately 50 μm as a balance among competing factors. A smaller path length minimizes the amount of background D_2O/buffer while a larger path length increases the absorbance of the sample and hence the change in absorbance. On the other hand, too large a path length reduces the total amount of light through the sample, and this increases the noise level. Sample concentrations of approximately 1 mN were employed (more concentrated solutions were unstable in the T-jump spectrometer showing substantial cavitations and showing evidence of precipitation), which yielded an absorbance of about 0.8 OD unit at 1679 cm^{-1} through 50 μm path length of the sample, one of the important frequencies. Two types of experiments were performed. In one, the LDH/NAD-pyr

adduct sample was run against D_2O/buffer as reference. Secondly, to minimize protein background signals from the observed kinetics, LDH/NAD-pyr adduct sample was run against the LDH/NAD-[^{13}C]pyr adduct reference. The isotope-edited difference transient should null out the response of the protein and contain only the pyruvate signal. In well-balanced cells, this latter approach should yield the most accurate data.

It is expected that the C═O stretch mode of the LDH/NAD-pyr adduct will shift upward if H-bond patterns at the binding site are transiently disrupted by the T-jump while the antisymmetric stretch mode of the −COO$^-$ moiety shifts downward (the directions observed as the pyruvate moiety dissociates from LDH; Figure 6). In this case, IR transient experiments at 1666 and 1676 cm^{-1}, the positions of bands with significant C═O stretch character (or at 1641 and 1652 cm^{-1} for ^{13}C2═O-labeled compounds), directly show a loss of intensity if there is any transient formation of a species with a disrupted H-bond interaction with the C═O group. Also, measurements at the edge of these bands would be sensitive to small shifts in frequency. The same is true for the −COO$^-$ antisymmetric stretch mode whose band lies at 1635 cm^{-1} (or 1609 cm^{-1} for the ^{13}C1OO$^-$-labeled compound) in the LDH/NAD-pyr adduct. The following measurements were performed (frequency and T-jump): 1696 cm^{-1} (6−19 °C and 26−40 °C), 1679 cm^{-1} (6−19 °C and 26−40 °C, 37−51 °C, 45−59 °C), 1665 cm^{-1} (30.4−40 °C and 35.7−44 °C), 1656 cm^{-1} (36.7−48 °C), 1634 cm^{-1} (36.7−50 °C), 1624 cm^{-1} (36.7−50 °C), 1608 cm^{-1} (6−19 °C), 1596 cm^{-1} (6−19 °C), and 1586 cm^{-1} (25.6−42.6 °C and 36.9−48.2 °C). All of these experiments yielded less than 0.5−1.0 mOD change in the amplitudes over the entire time range apart from the 40 ns transient (which includes the 23 ns instrument response) that is assigned to a protein response as found in the experiments shown in Figure 7.

Figure 8a shows a subset of these experiments: isotope-edited transients taken at four probe frequencies, at 1696 and 1679 cm^{-1}, designed to probe the response of the C═O stretch mode, and at 1608 and 1596 cm^{-1}, designed to probe the −COO$^-$ coordinate. The sample side of these runs contains LDH/NAD-pyr while the reference side contained LDH/NAD-[^{13}C1,^{13}C2]pyr. Panel b of Figure 8 graphs the difference between sample side minus reference side spectra. The reference data have been scaled according to the concentration ratio between the two sides of the split cuvette. The isotope- edited difference transients of Figure 8b are almost zero; they are all less than 0.5 mOD across the entire range in time except at the two ends, below 100 ns and above 2 ms. In various experiments, these "edge" transients varied from positive going signals to negative going signals. They arise from a small incomplete subtraction of the sample and reference signals that are expected from imperfectly matched sample conditions. The temperature jump of Figure 8 is 13 °C, from 6 to 19 °C.

For the data of Figure 8, the total protein optical absorbancy on the sample side is 561 mOD and on the reference side is 782 mOD. They are very concentrated samples. Using the data of Figure 6, the OD of the C═O stretch mode at 1676 cm^{-1}, scaled for concentration and path length, would be 14 and 19 mOD, respectively, and that of the 1635 cm^{-1} −COO$^-$ antisymmetric stretch mode would be 18 and 25 mOD, respectively. The scale of Figure 8b has been set so

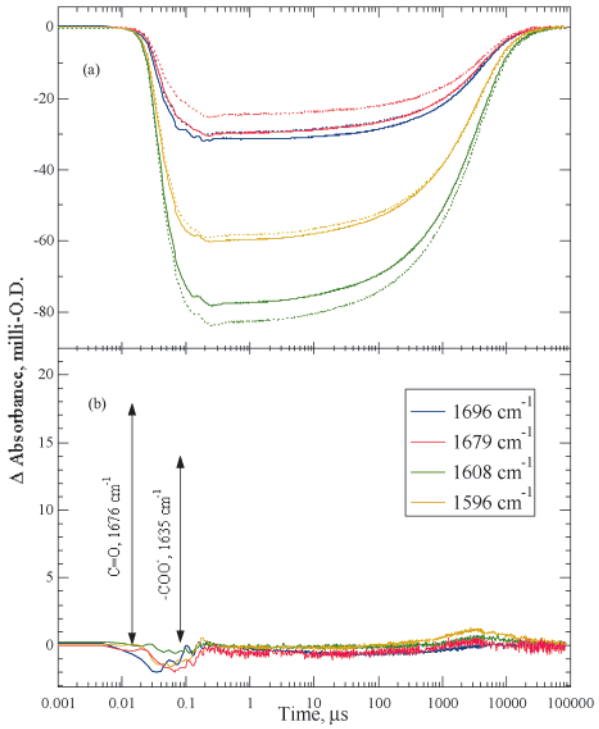

FIGURE 8: (a) Kinetic IR response of LDH/NAD-pyr in 5 mM deuterated sodium phosphate buffer, pH* = 7.0, for a T-jump from 6 to 19 °C at 1608, 1596, 1679, and 1696 cm^{-1} for LDH/NAD-pyr (sample side, dashed line) and LDH/NAD-[^{13}C1,^{13}C2]pyr (reference side, solid lines). The path length is 50 μm. The total protein optical absorbance at 1652 cm^{-1} (the amide peak of LDH) is 561 mOD, sample side, and 782 mOD, reference. (b) Difference transients formed by taking the difference between sample and reference signals where the two responses have been scaled to take into account the difference in concentration. The vertical bars represent the peak absorption of the C═O and −COO$^-$ stretch bands at 1676 and 1635 cm^{-1}, respectively, of the LDH/NAD-pyr adduct as deduced from the data of Figure 6 scaled for path length and concentration.

that these values are shown in vertical bars. It is clear that there has been no measurable response at any of the key frequencies marking the position of the adduct's C═O stretch or the antisymmetric −COO$^-$ stretch. For example, taking 14 mOD at the maximum of the C═O stretch at 1676 cm^{-1} and an observed response of less than 0.5 mOD yields no change in the peak position to within 28/1. From the data of Figure 6b, a shift of less than 1.5 cm^{-1} in the 1676 cm^{-1} band toward higher frequency would have yielded a measurable response. At 1696 cm^{-1}, had the C═O band shifted upward 11 cm^{-1}, as has been determined from static measurements if the loop containing Arg-109 opens and the C═O···Arg-109 is broken (*9*), a transient of 7 mOD would be expected. The numbers for the antisymmetric COO$^-$ stretch mode are similar. A downward shift of less than 0.3 cm^{-1} in the ^{13}COO$^-$ stretch at 1609 cm^{-1}, due for example to relative motion of Arg-171 against the ionized carboxylic moiety of pyruvate, would have yielded a 0.5 mOD response at this frequency.

DISCUSSION

T-jump relaxation spectroscopy perturbs the equilibrium point of interconverting chemical species by rapidly changing

the temperature, forcing the system to establish a new equilibrium point. The spectrometers used here heat water by pumping weak water absorption bands in the near-IR and employ fluorescence and mid-IR as probes of structure. For these systems, the time evolution of reaching the new equilibrium point is determined with a resolution of about 15 ns. The technique relies on the existence of an enthalpic difference between the old and new equilibrium points. It can be shown (*22*) that the change in equilibrium between two interconverting species for a given jump temperature is given by

$$\Delta K/K = (5.67 \times 10^3)\Delta H \Delta T$$

where K is the equilibrium constant, ΔH is the enthalpy difference between the two species (in kilocalories per mole), and ΔT is the temperature jump (in degrees kelvin). Our average T-jump is 15 °C, and our sensitivity to changes in K in the present experiments is approximately $\Delta K/K = 0.04$ or better. This implies that any two states separated by as little as 0.5 kcal/mol in enthalpy will be observed. The polar interactions at the binding site of LDH between protein and substrate involve substantially larger enthalpic interactions than this, as discussed below. For example, the binding enthalpy of pyruvate or the inhibitor oxamate to LDH/NADH is 15−18 kcal/mol (*23*). Hence, LDH is an appropriate system for T-jump relaxation spectroscopy in an examination of its catalytic dynamics.

We begin this discussion by asking what type of dynamics we might expect to occur. In general, we might expect any protein complex to adopt a range of conformational substates, with these substates possessing a range of functional efficacy. For example, it has been observed that the binding of NADH to LDH is a multistep process, with dynamics observed on multiple time scales from nanoseconds to milliseconds (*17*). It was found that the LDH/NADH complex does not adopt a single structure. The binary complex adopts multiple interconverting structures of significant population; some of these structures appear to be far from catalytically productive. Hence, one important question in the present study is whether the ternary protein/cofactor/substrate complex also consists of multiple interconverting structures, and if so, are some of these either catalytically nonproductive or less productive compared to others. This possibility is reinforced by our recent observation (unpublished data) that multiple vibrational bands indicating multiple populated conformations are observed for the catalytically key C4−H stretch coordinate of NADH bound as the LDH/NADH/oxamate complex, with theoretical considerations suggesting that only one of these species can be close to the productive geometry. Moreover, the C═O stretch mode of the bound pyruvate moiety of the NAD-pyr adduct is quite broad (see Results), some of which may be the result of a heterogeneous broadening mechanism brought about by a distribution of interactions at the binding site. Clearly heterogeneously broadened bands for the C═O stretch of the bound pyruvate moiety when bound to mutants of LDH have been observed (*9*). Since the C═O stretch frequency is a direct monitor of k_{cat}, with a 34 cm^{-1} shift corresponding to a factor of $10^{5.5}$ rate enhancement of the hydride transfer (*9*), a particular substrate's catalytic efficiency can be assessed if the frequency distribution of the heterogeneous ensemble is determined.

The known characteristic relaxation rates of loop closure/opening when substrate binds to the LDH/NADH binary complex are 3600 s^{-1} at 23 °C (*11*) and 8400 s^{-1} at 41 °C (see Results). The structural event that is being monitored on these time scales is one that quenches the fluorescence quantum yield of the reduced nicotinamide ring as the ring closes over the binding site. This is probably the last event, or very close to the last event, in the process of loop closure since it is well-known that the emission of NADH in the "closed" ternary LDH/NADH/substrate ternary complex is almost completely quenched. Loop closure is of substantial importance to the chemistry of catalysis in LDH; it enhances k_{cat} in LDH by over a factor 1200 (*24*). For a simple model of the dynamics that involves the loop closing over the substrate binding site with substrate more or less in place, the kinetics of loop closure should be observed in experiments on the LDH/NAD-pyr adduct complex since the frequency of the adduct's C═O stretch shifts substantially upward upon loop opening (*9*).

Finally, the local energies of the hydrogen bonds between various groups of LDH and the C═O group of the NAD-pyr adduct have been deduced from their effect of polarizing the C═O bond through shifts in the C═O stretch mode of the pyruvate moiety of the bound NAD-pyr adduct (*9*). The values are 11 and 4 kcal/mol between the C═O group and the key active site His-195/Asp-168 dyad and the loop containing Arg-109, respectively. The breaking of the C═O···Arg-109 H-bond is clearly not too difficult and may be expected to break and form many times during the ca. 1 ms time that it takes for catalytic chemistry to occur in LDH. The breaking of the C═O···His-195 bond, although substantial, may well also occur. For example, using a Boltzman distribution that describes the thermal population of states and a preexponential factor of 10^{13} s^{-1}, it is predicted that the C═O···His-195 bond will break in about 10 μs.

To focus on the dynamics occurring at the binding site of LDH once substrate is bound, we have performed studies on the LDH/NAD-pyr complex. The actual process of forming an encounter complex in the binding of substrate to enzyme has already occurred so that these dynamics are "frozen out". Substrate binding dynamics can be studied separately in experiments, for example, of the binding of the inhibitor oxamate to LDH/NADH (*10*, *11*; see Results). Furthermore, the LDH/NAD-pyr adduct is unable to undergo hydride transfer so that the kinetics associated with the chemistry transforming substrate to product do not complicate the interpretations of the results. The LDH/NAD-pyr adduct is not a strict mimic of the ground-state Michaelis complex. The structural arrangement and interactions of the carboxyl and carbonyl groups of the pyruvate moiety of the NAD-pyr adduct with its protein environment when bound to LDH are believed to mimic quite well what would be encountered with a true Michaelis ground-state LDH/NADH/pyruvate ternary complex (*1*−*9*). On the other hand, the NAD cofactor is covalently bound to the pyruvate substrate, and the two molecules which would normally react at the active site are kept close to each other.

The results on the LDH/NAD-pyr adduct complex show no dynamical features from 20 ns to out to at least the millisecond time scale apart from the "melting" of a few residues on the protein's surface and, hence, none that would affect catalysis over this time scale. The experiments are quite

sensitive. Virtually any change in the distances between the pyruvate group's C═O bond and −COO^- group with regard to the key active site residues His-195, Asp-168, Arg-109, and/or Arg-171 would have shown up as shifts in the C═O or −COO^- stretch bands. No shifts were observed with a sensitivity of around 30/1. It should be noted that our experiments reached a final temperature near 50 °C, which is close to the unfolding temperature of LDH (T_m = 62 °C in the rabbit muscle protein; *25*). We conclude that the active site groups in LDH around the pyruvate moiety of the NAD-pyr adduct are quite immobilized and rigid. If there are populated protein substates which include a different geometric arrangement of the polar groups at LDH's active site, the enthalpy difference between them is less than 0.5 kcal/mol or less than the 0.6 kcal thermal energy at room temperature. Given the strengths of the various hydrogen bonds at the active site and the sizable enthalpies involved in these bonds, there would appear to be virtually no distribution of substrates that involve perturbations of these bonds.

A surprising result of this study is the lack of any kinetics associated with loop closure in the LDH/NAD-pyr complex which was shown in Results to occur at 119 μs (at 41 °C) in experiments of the binding of oxamate to LDH/NADH. A simple binding model would have the substrate enter into the active site with the mobile loop in an open conformation. Once the substrate orientates itself within the binding pocket, the loop closes over the substrate. In the reverse of this process, the mobile loop breaks contact with substrate in the LDH/NADH/pyruvate ternary complex, breaking among other interactions the H-bond between C═O···Arg-109, followed by the leaving of the substrate. The present results show that this model cannot describe the dynamics of loop motion given that no changes in the C═O stretch mode were observed in the LDH/NAD-pyr complex. The formation of the adduct complex, which ties the pyruvate moiety to the binding site because it is covalently linked to bound NAD, clearly greatly slows loop opening (to a time where we cannot observe it). It can be concluded from our Results that the simple model described above cannot describe loop dynamics but rather points to loop opening motion that involves a coordinated motion of the substrate as well as the loop. It is clear that the substrate must move either with or in some partial way with the protein loop. The kinetics of product release from LDH appear to rely on a small substrate and its concomitant mobility. Conversely, the process of substrate binding to the enzyme may depend on forming an encounter complex between the open loop enzyme and substrate.

REFERENCES

1. Burgner, J. W., and Ray, W. J. (1984) *Biochemistry 23*, 3636−3648.
2. Holbrook, J. J., Liljas, A., Steindel, S. J., and Rossmann, M. G. (1975) in *The Enzymes* (Boyer, P. D., Ed.) pp 191−293, Academic Press, New York.
3. White, J. L., Hackert, M. L., Buehner, M., Adams, M. J., Ford, G. C., Lentz, P. J., Smiley, I. E., Steindel, S. J., and Rossmann, M. G. (1976) *J. Mol. Biol. 102*, 759−779.
4. Grau, U. M., Trommer, W. E., and Rossmann, M. G. (1981) *J. Mol. Biol. 151*, 289−307.
5. Wigley, D. B., Gamblin, S. J., Turkenburg, J. P., Dodson, E. J., Piontek, K., Muirhead, H., and Holbrook, J. J. (1992) *J. Mol. Biol. 223*, 317−335.
6. Burgner, J. W., and Ray, W. J. (1984) *Biochemistry 23*, 3620−3626.
7. Burgner, J. W., and Ray, W. J. (1984) *Biochemistry 23*, 3626−3635.
8. Deng, H., Zheng, J., Burgner, J., and Callender, R. (1989) *Proc. Natl. Acad. Sci. U.S.A. 86*, 4484−4488.
9. Deng, H., Zheng, J., Clarke, A., Holbrook, J. J., Callender, R., and Burgner, J. W. (1994) *Biochemistry 33*, 2297−2305.
10. Clarke, A. R., Waldman, A. D. B., Hart, K. W., and Holbrook, J. J. (1985) *Biochim. Biophys. Acta S29*, 397−407.
11. Parker, D. M., Jeckel, D., and Holbrook, J. J. (1982) *Biochem. J. 201*, 465−471.
12. Burgner, J. W., and Ray, W. J. (1974) *Biochemistry 13*, 4229−4237.
13. Cheng, H., Sukal, S., Deng, H., Leyh, T. S., and Callender, R. (2001) *Biochemistry 40*, 4035−4043.
14. Williams, S., Causgrove, T. P., Gilmanshin, R., Fang, K. S., Callender, R., Woodruff, W., and Dyer, R. B. (1996) *Biochemistry 35*, 691−697.
15. Gilmanshin, R., Williams, S., Callender, R. H., Woodruff, W., and Dyer, R. B. (1997) *Proc. Natl. Acad. Sci. U.S.A. 94*, 3709−3713.
16. Dyer, R. B., Gai, F., Woodruff, W., Gilmanshin, R., and Callender, R. H. (1998) *Acc. Chem. Res. 31*, 709−716.
17. Deng, H., Zhadin, N., and Callender, R. (2001) *Biochemistry 40*, 3767−3773.
18. Gulotta, M., Gilmanshin, R., Callender, R. H., and Dyer, R. B. (2001) *Biochemistry 40*, 5137−5143.
19. Puustinen, A., Bailey, J. A., Dyer, R. B., Mecklenburg, S. L., Wikstrom, M., and Woodruff, W. H. (1997) *Biochemistry 36*, 13195−13200.
20. Thompson, P. A., Eaton, W. A., and Hofrichter, J. (1997) *Biochemistry 36*, 9200−9210.
21. Gu, Z., Zambrano, R., and McDermott, A. (1994) *J. Am. Chem. Soc. 116*, 6368−6372.
22. Bernasconi, C. F. (1976) *Relaxation Kinetics*, Academic Press, New York.
23. Schmid, F., Hinz, H.-J., and Jaenicke, R. (1976) *Biochemistry 15*, 3052−3059.
24. Clarke, A. R., Wigley, D. B., Chia, W. N., and Holbrook, J. J. (1986) *Nature 324*, 699−702.
25. Jacobson, A. L., and Braun, H. (1977) *Biochim. Biophys. Acta 493*, 142−153.

BI016009A